A cartographic study of the phase space of the restricted three body problem

C. Galeş*

**Faculty of Mathematics, Al. I. Cuza University of Iaşi, Blvd. Carol I, no. 11, 700506 Iaşi, Romania (Tel: +40742258476; e-mail: cgales@uaic.ro).*

Abstract: This work deals with numerical investigations of the phase space of the restricted three body model. The Sun-Jupiter-Asteroid system is considered and the fast Lyapunov indicator (FLI) is used as a tool to examine various types of orbits on which the infinitesimal mass can undergo. The FLI is computed on given grids of initial conditions and the obtained charts are analyzed. The chaotic zones and the libration regions associated with the mean motion resonances of low order are clearly distinguished. Their size is discussed as a function of the resonance order and the parameters entering into the perturbing function.

Keywords**:** Phase space, Numerical methods, Dynamics, Resonance, Chaotic behaviour.

1. INTRODUCTION

In the last two decades, various numerical methods have been applied to celestial mechanics to distinguish between regular and chaotic motions. Depending on the mathematical model, the information offered and the amount of computation, each method has its own advantages and disadvantages. We shall briefly recall some widely used tools in investigating the dynamics of non-integrable systems. Thus, the frequency map analysis (Laskar, 1990; Laskar *et al.*, 1992) has been used for studying small body dynamics (Nesvorný and Ferraz-Mello, 1997; Celletti *et al.*, 2004); the method of twist angles (Contopoulos and Voglis, 1997) has been tested on the standard map and compared with other methods of analysis (Froeschlé and Lega, 1998); the fast Lyapunov indicator (Froeschlé *et al.*, 1997a, 1997b) has been investigated in detail and applied to various dynamical problems; the MEGNO technique (Cincotta and Simó, 2000) has been utilized to perform a stability analysis of extra solar planets (Goździewski *et al.*, 2001; Goździewski, 2003); the time series given by the intervals between successive crossing of a given plane of section have been used to reconstruct the phase space in the restricted three body problem (Gidea *et al.*, 2007).

In this paper, we use the fast Lyapunov indicator (FLI) in order to perform a cartographic study of a given portion of the phase space of the restricted three body problem. Introduced by Froeschlé *et al.* (1997a, 1997b), this tool is easy to implement, cheap in computational time and very sensitive for the detection of weak chaos and for distinguishing between regular resonant orbits and regular non resonant ones. These features have been unveiled by testing it on symplectic mappings (Froeschlé and Lega, 2000a; Lega and Froeschlé, 2001) as well as on continuous flows (Fouchard *et al.,* 2002). Moreover, it was shown that FLI is a very useful numerical tool for revealing the geometry of resonances (the so-called Arnold's web), for detecting the transition between the stable Nekhoroshev's regime and the diffusive Chirikov's one (Froeschlé *et al.*, 2000b; Guzzo *et al.*, 2002; Todorović *et al.*, 2008) and even for detection of diffusion along resonances (Arnold's diffusion) (Lega *et al.*, 2003, 2008; Froeschlé *et al.*, 2006; Todorović *et al.*, 2008). These topics have been investigated in the framework of quasi-integrable Hamiltonian systems. In this sense, some model systems have been carefully chosen.

The FLI tool has been directly utilized to study the stability of extra solar planets (Pilat-Lohinger, 2003), to solve spacecraft preliminary trajectory design problems (Villac, 2008), to investigate the dynamics associated to nearly integrable dissipative systems (Celletti, 2008).

In this paper, we use the FLI tool to investigate the phase space of the restricted three body problem and we focus on the Sun-Jupiter-Asteroid system. We recall that FLI has been first applied to asteroidal motion. Froeschlé *et al.* (1997b) integrated a model consisting of the four giant planets and Sun and studied the dynamics of the asteroids orbiting between the 3/1 and 5/2 Kirkwood gaps. Here, we implement the FLI tool for the elliptic restricted three body model (the case Sun-Jupiter-infinitesimal mass) and prove that FLI reveals after a very short computational time the entire structure of the phase space (the regular and chaotic regions, the geometry of resonances, the libration regions).

This analysis is relevant in the study of the global dynamics in the asteroid belt. This topic, with a particular attention on the mechanisms of chaotic diffusion, is extensively studied in literature (see for example the book of Morbidelli (2002) and the review article by Tsiganis (2008)). The theories of chaotic diffusion aim to predict the long-term behaviour of ensembles of asteroids, rather than individual orbits. In this sense, the Lyapunov time, the size and shape of the chaotic regions and the diffusion coefficients are the main parameters needed to understand the long-terms effect of chaotic diffusion in the asteroid belt. To compute them, analytical models and numerical studies of two-body mean motion resonances of different order have been accomplished

(Holman and Murray, 1996; Murray and Holman, 1996; Morbidelli, 2002; Tsiganis, 2008; and references therein).

Here, a numerical study is given in the framework of the planar elliptic restricted three body problem in order to give an estimate of the size and the shape of the chaotic regions. We integrate the variational equations along with the equations of motion for a set of *500 x 500* test particles placed on a regular grid in the plane *(a, e)*, where the semi-major axis a range from *1.5* AU to *6* AU, while the eccentricity $e \in [0, 0.5]$. The total time span covered by our integration has a length of *8400* yr (*700* periods of Jupiter). On the obtained dynamical maps, the structure of the above portion of the phase space is clearly displayed.

In contrast with other numerical methods, for example with the classical method for detecting chaotic behaviour in asteroid belt, which is that of the Lyapunov exponents, the FLI is computationally cheap and robust. Here, the integration time is of 10^3-10^4 yr. To compute a dynamical map using the maximum Lyapunov exponent the integration time is of the order of millions of yr (Tsiganis, 2008).

2. BASIC FORMULATION

In this section we recall the definition of the FLI and we describe the techniques utilized to integrate the equations of motion and the variational equations.

2.1 The fast Lyapunov indicator (FLI)

Let us consider the dynamical system

$$dX/dt = F(X(t)), \qquad X \in R^n, \quad t \in R, \tag{1}$$

where F is a continuously differentiable function. Given an initial condition $X(0) \in R^n$, let us consider the evolution $V(t) \in R^n$ of an initial vector $V(0) \in R^n$ of norm *1*, obtained by integrating the variational equations

$$\frac{dV}{dt} = \frac{\partial F}{\partial X}(X(t))V, \tag{2}$$

where $X(t)$ is the evolution of $X(0)$.

Then, the maximum Lyapunov exponent is defined by

$$MLE(X(0)) = \lim_{t\to\infty}[(\ln\|V(t)\|)/t]. \tag{3}$$

Numerically, one works on finite times. Thus, one estimates *MLE* by computing the Lyapunov characteristic indicator defined by

$$LCI(t; X(0)) = (\ln\|V(t)\|)/t \tag{4}$$

at a large time t.

The fast Lyapunov indicator is defined by (Froeschlé and Lega, 2000a; Lega and Froeschlé 2001)

$$FLI(T; X(0)) = \sup_{0<t<T} \ln\|V(t)\|. \tag{5}$$

The computation of FLI on a relatively short time is enough to discriminate between chaotic and regular orbits. The FLI of a regular orbit increases linearly, while for a chaotic orbit, the FLI increases exponentially. Moreover, FLI may be used to discriminate among regular motion between non resonant and resonant orbits. Because of the differential rotation, the norm of the vector V, asymptotically grows as $\|V(t)\| \cong at$, the coefficient a depending on the nature of invariant curve (torus or libration island). As against the MLE, there is a disadvantage. Namely, FLI depends on the initial conditions and if the system is Hamiltonian, on the choice of the canonical variables. But, once some reference orbits have been computed for which the chaotic (or regular) nature has been determined, the FLI allows the investigation of a large number of orbits.

2.2 The restricted three body problem

The three-body problem simplified by setting one mass to zero is widely known as the restricted three-body problem. In this case the equations for the two primaries S (Sun) and J (Jupiter) decouple, so that their motion is Keplerian. According to the value of the eccentricity of their orbits we speak of the circular or elliptic problem. Here we consider the elliptic problem.

We define our system of units such that $G\,(m_S+m_J)=1$, where G denotes the constant of gravitation, m_S the mass of the Sun, m_J the mass of Jupiter. Let us introduce the notation

$$\mu = Gm_J = m_J/(m_S + m_J) = 9.54 \cdot 10^{-4}. \tag{6}$$

Then, the heliocentric equations of motion of Jupiter and the infinitesimal body are

$$\begin{aligned} &d^2\vec{r}_J/dt^2 = -\vec{r}_J/\|\vec{r}_J\|^3, \\ &d^2\vec{r}/dt^2 = -(1-\mu)\,\vec{r}/\|\vec{r}\|^3 \\ &\qquad + \mu[(\vec{r}_J - \vec{r})/\|\vec{r}_J - \vec{r}\|^3 - \vec{r}_J/\|\vec{r}_J\|^3], \end{aligned} \tag{7}$$

where $\vec{r}_J$ and $\vec{r}$ are their position vectors relative to the Sun.

We have numerically integrated the above equations using as starter a single step method (Runge-Kutta), while a symmetric multistep method of 12th order (Quinlan and Tremaine, 1990) performs most of the propagation. For the corresponding variational equations, we have utilized again the Runge-Kutta method. For each initial condition, the total time span covered by the integration has a length of *8400* yr (*700* periods of Jupiter). The computations for a longer time (over 1000 periods of Jupiter) did not change the result significantly, therefore we used a shorter computation time for the whole analysis. The initial conditions have been chosen such that the second primary (Jupiter) describes an elliptic motion with eccentricity $e_J = 0.048$ and at time $t=0$, Jupiter is at perihelion. We have utilized a Cartesian coordinate system centred on the Sun with the x axis pointing towards the perihelion of Jupiter.

We suppose the massless body moves in a coplanar heliocentric elliptic orbit perturbed by Jupiter. Its initial conditions are given once the semi-major axis a (in AU), the eccentricity e, the argument of perihelion ω (the angle between the perihelion line and the x line) and the mean anomaly M are prescribed.

In order to exemplify the behaviour of FLI for different kind of orbits, we plotted the evolution of the values of FLI for four orbits: O_1 (regular orbit), O_2 (regular resonant orbit), O_3 (weak chaotic orbit) and O_4 (strong chaotic orbit) during 1000 periods of Jupiter (see Fig. 1). The orbits correspond to the following initial conditions: O_1: $a=2.43$AU, $e=0.15$, $\omega=0$, $M=0$; O_2: $a=2.49$ AU, $e=0.15$, $\omega=0$, $M=0$; O_3: $a=2.53$ AU, $e=0.15$, $\omega=0$, $M=0$; and O_4: $a=4.7$ AU, $e=0.15$, $\omega=0$, $M=0$. The regular orbit O_1 is close to the 3:1 resonance, O_2 is in the libration region of the 3:1 resonance, O_3 is on the separatrix of the 3:1 resonance, while O_4 is located in the unstable region (see Fig. 3A). For the regular orbits O_1 and O_2, FLI increases linearly. The FLI of the chaotic orbits O_3 and O_4 increases exponentially, but with different rates.

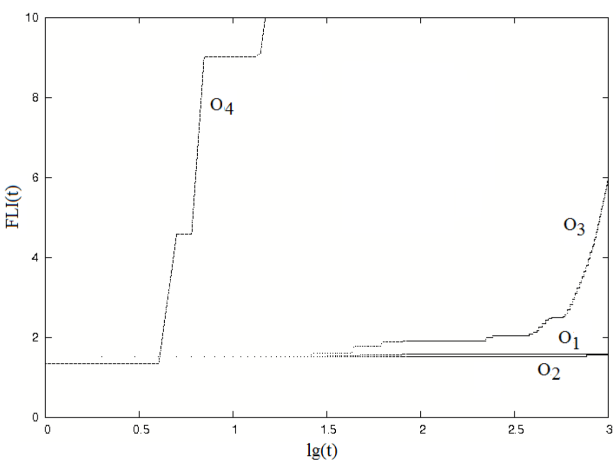

Fig. 1. Evolution of FLI as a function of $lg(t)$ for the orbits: O_1 (regular orbit), O_2 (regular resonant orbit), O_3 (weak chaotic orbit) and O_4 (strong chaotic orbit). The unit of time is the period of Jupiter

3. RESULTS

In this Section we describe numerically the structure of a given portion of the phase space of the planar elliptic restricted three body problem (PERTBP) by computing dynamical maps, such as the ones presented in Fig. 3. In order to give a theoretically based interpretation to our numerical analysis we recall first some important definitions and analytical results.

The phase space of the PERTBP is four dimensional. Thus, from a theoretical point of view, to describe a portion of it, a dense network of points covering a subset of R^4 should be investigated. However, since our model is a quasi-integrable Hamiltonian system, we resort to the space of the actions.

In the case of quasi-integrable Hamiltonian systems having a non-degenerate integrable part, the KAM theorem (see for example Celletti and Chierchia (2006) for a recent description of the state of the art of the theory) assures the persistence of invariant tori carrying motion with diophantine frequencies, provided the perturbations are small enough. In other words, the non-degenerate integrable approximation H_0 gives a foliation of the phase space in invariant tori, the actions being constants and the angles circulating linearly with time. When a small perturbation εH_1 is added, the KAM theorem ensures that some invariant tori with diophantine frequencies continue to be invariant for the complete Hamiltonian $H_0 + \varepsilon H_1$. The size ε determines which tori continue to be invariant among all the unperturbed ones with diophantine frequencies.

Clearly, the integrable part of the PRTBP, namely the two body problem is highly degenerate and the hypotheses of the KAM theorem are not satisfied. For this reason the PRTBP exhibit very complicated dynamics. In the phase space, we identify: regular regions, chaotic areas and resonant regions with its libration and chaotic zones.

Let us recall now the Hamiltonian and the canonical variables of the planar restricted three body problem. With our choice of dimensions and the Cartesian coordinate system, the modified Delaunay variables are

$$\begin{aligned} \Lambda &= \sqrt{(1-\mu)a}\,, & \lambda &= M + \omega\,, \\ \Omega &= \Lambda(1-\sqrt{1-e^2})\,, & &-\omega\,. \end{aligned} \tag{8}$$

The autonomous Hamiltonian has the form

$$\begin{aligned} H = -(1-\mu)^2/(2\Lambda^2) + n_J\Lambda_J \\ - \mu f(\Lambda, \Omega, \lambda, \omega, \lambda_J), \end{aligned} \tag{9}$$

where $n_J = \dot{\lambda}_J$ is the mean motion of Jupiter, λ_J is the mean longitude and Λ_J is the conjugate action corresponding to Jupiter. The disturbing function f, also depends on the constant elements of Jupiter's orbit (for a detailed description of the perturbation theories the reader is referred to the books of Murray and Dermott (1999) and Ferraz-Mello (2007)). The integrable part of H is degenerate. The angle λ is non-degenerate, while ω is degenerate.

Now, we recall that the resonances

$$(p+q)\dot{\lambda} - p\dot{\lambda}_J = 0\,, \quad p, q \in Z \tag{10}$$

are called mean motion resonances. q is the order of resonance and determines its strength. It is known that asteroids can develop chaotic motion as a result of resonant perturbations, exerted by the major planets. The asteroid-Jupiter mean motion resonances of low order ($2 \le q \le 4$) force the resonant asteroids to become planet crossers on a short timescale (of order of a few million years), while in mean motion resonances of moderate order ($5 \le q \le 7$-9) the times required to become a planet crosser are much longer (from tens of millions of years to of order 1 Gyr) (see Morbidelli (2002)).

In order to investigate numerically the topology of the phase space, we proceeded as follows: in the domain $0 \le e \le 0.5$, 1.5 AU $\le a \le 6$ AU, of the action plane (Λ, Ω) we considered a grid of *500 x 500* equidistant initial conditions. The choice of initial angles was: A) *ω=0, M=0; B) ω=90, M=0; C) ω=180, M=0; D) ω=60, M=0; E) ω=-60, M=0*; For each point on the grid we calculated the final value of the logarithm of FLI for 700 periods of Jupiter. The results are reported below (Fig. 3: A, B, C, D and E), where the grey scale is used in such a way that white colour corresponds to chaotic orbits, whereas the darker colour is, the more stable the orbit is.

Moreover, we represented the distribution of the main belt and Trojans asteroids (Fig. 2) using the osculating semi-major axis and eccentricity, in order to display the location of the mean motion resonances with Jupiter. We recall the location of some low order resonances: *4:1 (a=2.06* AU*); 3:1 (a=2.5*AU*); 5:2 (a=2.82* AU*); 7:3 (a=2.95* AU*); 2:1 (a=3.277* AU*); 7:4 (a=3.58* AU*); 5:3 (a=3.7* AU*); 3:2 (a=3.9* AU*); 1:1 (a=5.2* AU*)*.

Figs. 3 A, B, C, D and E are in a good agreement with the analytical and numerical studies on the global dynamics of asteroid belt (Murray and Dermott, 1999; Tsiganis, 2008; Morbidelli, 2002; and references therein). Analysing these maps we may conclude the followings: Depending on the initial proper elements *a*, *e*, *ω,* the infinitesimal mass can undergo chaotic or regular motions.

The *stability region*, located between 1.5 AU and 3.2 AU is clearly distinguished on each map. Moreover, the maps computed for *ω=60* and *ω=-60* (Figs. 3 D, E) show the regular zones associated with 1:1 jovian resonance.

The *strong chaotic motions* arise as a consequence of the resonance overlap criterion. This criterion was discussed by Wisdom (1980). One could consider the phase space as being made up of a succession of resonances, each independent of the others and having its own librational and chaotic regions, as in the case of the perturbed pendulum. An obvious example is the sequence of the first order interior resonances of the form *p+1:p.* Since each resonance has a well-defined width in semi-major axis, and since the separation of adiacent resonances becomes smaller as the perturber is approached, there will come a point at which these overlap (for example the resonances: 4:3 (*a=4.29*AU); 5:4 (*a=4.48*AU); 6:5 (*a=4.6*AU) etc.) As a consequence, we would expect a cleared zone in the asteroid belt beyond 4.3 AU. This is in good agreement with the observations (see Fig. 2). The chaotic zone predicted by the above described overlap criterion is obtained in each picture. For *a ≥ 4.3* a large white zone, whose shape depends on *ω,* is obtained by numerical integration.

The stability region is crossed by a series of 'V'-shaped layers of various sizes. These layers correspond to the *mean motion resonances* of low order (*4:1 (a=2.06* AU*); 3:1 (a=2.5*AU*); 5:2 (a=2.82* AU*); 7:3 (a=2.95* AU*); 2:1 (a=3.277* AU*); 7:4 (a=3.58* AU*); 5:3 (a=3.7* AU*);* see also the Fig. 2). Moreover, between *2.5* AU and *3.27* AU, we can distinguish very thin white lines which for high eccentricity overlap with the mean motion resonance of low order. These lines correspond to moderate-order mean motion resonances.

From a mathematical point of view, the dynamics inside mean motion resonances can be explained by analogy to perturbed pendulum. In the pendulum case the phase space has two regions, the libration and the circulation zones, separated by separatrix. When the perturbing function is taken into account the separatrix disappears. It place is taken by a chaotic region, whose size depends on the perturbation.

For each mean motion resonance of low order (see for example the resonance 3:1 (*a=2.5* AU), Fig. 3) we recognize its chaotic border (separatrix) and the libration region. Moreover, inside mean motion resonances we have other small chaotic lines, whose size and location depend again on *ω*. These regions are due by the contribution to the disturbing functions of the possible resonant arguments. Due to degeneracy of the problem each resonance splits into a multiplet of resonances. For example, the angles associated to the 3:1 resonance are $\varphi_1 = 3\lambda_J - \lambda - 2\omega$, $\varphi_2 = 3\lambda_J - \lambda - \omega - \omega_J$ and $\varphi_3 = 3\lambda_J - \lambda - 2\omega_J$. Since ω have a small but nonzero frequency, φ_1, φ_2 and φ_3 have zero derivatives at different locations. Therefore, the 3:1 mean motion resonance splits in a natural way into a threeplet of resonances. The exact location of each component is given by $\dot{\varphi}_k = 0$, *k=1,2,3.* The image of a given mean motion resonance varies from map to map since $\dot{\omega}$ depends on *ω* via Lagrange's equations.

Finally, we note that the libration region around mean motion resonance decreases with the order *q* and increases with the eccentricity *e*. In other words the layer around a mean motion resonance has a 'V'-shape and occupies smaller area once the order q increases. These results are in agreement with the analytical perturbation theory (Murray and Dermott, 1999), which guaranties higher terms in disturbing function once the order *q* is low and the eccentricity *e* is high. In fact, the coefficients of the resonant terms are proportional to e^q .

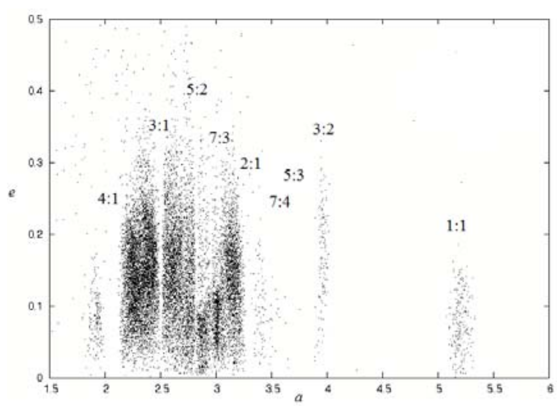

Fig. 2. Distribution of the main-belt and Trojans asteroids on the (*a, e*)-plane

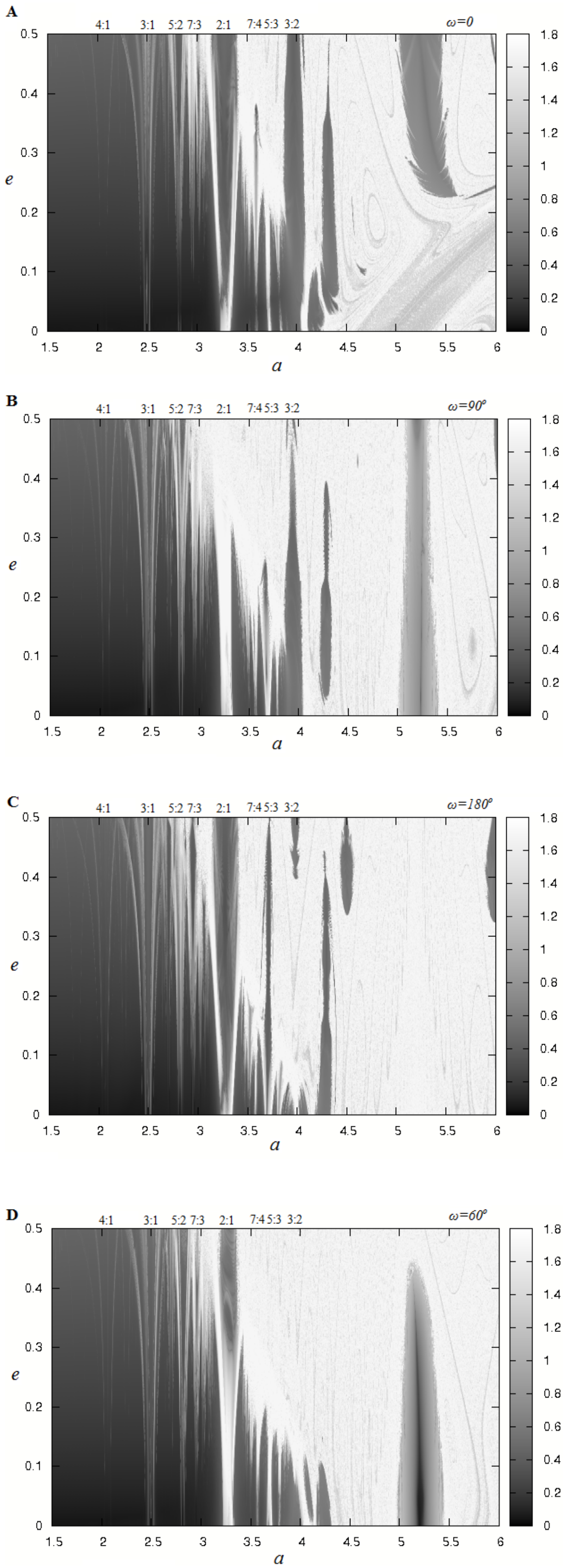

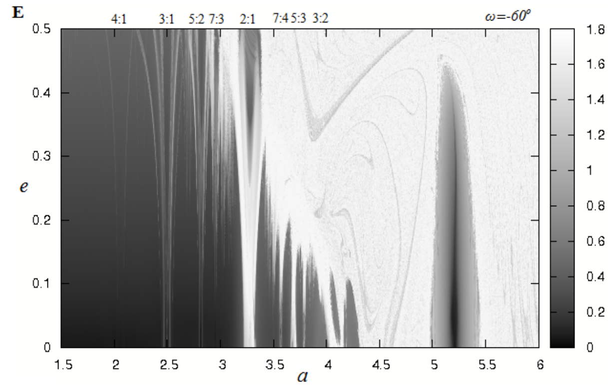

Fig. 3. Maps of the logarithm of the final value of FLI after 700 periods of Jupiter. The test particles were placed on a regular 500x500 grid in (a, e) plane and the initial angles was: A) ω=0, M=0; B) ω=90, M=0; C) ω=180, M=0; D) ω=60, M=0; E) ω=-60, M=0*;* The values of *lg(FLI)* are color-coded, according to the scale shown on the right (black=regular, white=chaotic)

4. CONCLUSIONS

The two body problem is highly degenerate. For this reason even small perturbations of the two-body problem, like the restricted three body problem, may exhibit very complicated dynamics. In this paper we considered the planar elliptic restricted three body problem (the Sun-Jupiter-Asteroid system) and by using the fast Lyapunov indicator we studied numerically the global topology of the phase space. On each dynamical map, regular regions, chaotic zones and 'V'-shaped layers around the mean motion resonances of low order, predicted by analytical theories (Murray and Dermott, 1999; Tsiganis, 2008; Morbidelli, 2002; and references therein) are revealed by the FLI in a very short computationally time. The degeneracy of the problem, pointed out by the resonance splitting, is clearly illustrated in the Figs. 3. Secular and mean-motion resonances of low order are known to lead to fast chaotic transport of asteroid orbits on million year time-scales (Gladman *et al.,* 1997; Morbidelli, 2002).

On our dynamical maps, some thin layers associated with mean motion resonances of moderate order are displayed. These resonances together with the three-body mean motion resonances (asteroid-Jupiter-Saturn) (Nesvorný and Morbidelli, 1998) form a dense network of thin chaotic layers throughout the asteroid belt, where small-amplitude variations of proper elements of asteroids accumulate slowly over time. This effect is known as chaotic diffusion (Tsiganis, 2008). The results obtained here for the PERTBP encourage the application of the FLI to study this fine chaotic structure of the asteroid belt.

Acknowledgements. This work was supported from the POSDRU/89/1.5/S/49944 Project.

REFERENCES

Celletti, A., C. Froeschlé and E. Lega (2004). Frequency analysis of the stability of asteroids in the framework of the restricted three-body problem. *Celest. Mech. Dynamical Astron.*, **90**, 245-266.

Celletti, A. and L. Chierchia (2006). KAM tori for N-body problems (a brief history). *Celest. Mech. Dynamical Astron.*, **95**, 117-139.

Celletti, A. (2008). Weakly dissipative systems in Celestial Mechancs. *Lect. Notes Phys.,* **729**, 67-90.

Cincotta, P. and C. Simó (2000). Simple tools to study global dynamics in non-axisymetric galactic potentials-I. *Astron. Astrophys. Suppl. Ser.*, **147**, 205-228.

Contopoulos, G. and N. Voglis (1997). A fast method for distinguishing between order and chaotic orbits. *Astron. Astrophys.*, **317**, 73-81.

Ferraz-Mello, S. (2007). Canonical perturbations theories. Degenerate systems and resonance. Springer, New York.

Fouchard, M., E. Lega, Ch. Froeschlé and C. Froeschlé (2002). On the relationship between fast Lyapunov indicator and periodic orbits for continuous flows. *Celest. Mech. Dynamical Astron.*, **83**, 205-222.

Froeschlé, C., E. Lega and R. Gonczi (1997a). Fast Lyapunov indicators. Application to asteroidal motion. *Celest. Mech. Dynamical Astron.*, **67**, 41-62.

Froeschlé, C., R. Gonczi and E. Lega (1997b). The fast Lyapunov indicator: a simple tool to detect weak chaos. Application to the structure of the main asteroidal belt. *Planet. Space Sci.*, **45**, 881-886.

Froeschlé, C. and E. Lega (1998). Twist angles: a method for distinguishing islands, tori and weak chaotic orbits. Comparison with other methods of analysis. *Astron. Astrophys.*, **334**, 355-362.

Froeschlé, C. and E. Lega (2000a). On the structure of symplectic mappings. The fast Lyapunov indicator: a very sensitive tool. *Celest. Mech. Dynamical Astron.*, **78**, 167-195.

Froeschlé, C., M. Guzzo and E. Lega (2000b). Graphical evolution of the Arnold web: from order to chaos. *Science*, **289**, 2108-2110.

Froeschlé, C., M. Guzzo and E. Lega (2006). Analysis of the chaotic behaviour of orbits diffusing along the Arnold web. *Celest. Mech. Dynamical Astron.*, **95**, 141-153.

Gidea, M., F. Deppe and G. Anderson (2007). Phase space reconstruction in the restricted three-body problem. In: *New Trends in Astrodynamics and Applications III* (Eds. E. Belbruno), AIP Conference Proceedings Volume 886.

Gladman, B. et al. (1997). Dynamical lifetime of objects injected into asteroid belt resonances. *Science*, **277**, 197-201.

Goździewski, K. (2003). A dynamical analysis of the HD 37124 planetary system. *Astron. Astrophys*., **398**, 315-325.

Goździewski, K., E. Bois, A.J. Maciejewski, L. Kiseleva-Eggleton (2001). Global dynamics of planetary systems with the MEGNO criterion. *Astron. Astrophys*., **378**, 569-586.

Guzzo, M., E. Lega and C. Froeschlé (2002). On the numerical detection of the effective stability of chaotic motions in quasi-integrable systems. *Physica D*, **163**, 1-25.

Holman, M. and N. Murray (1996). Chaos in high order mean motion resonances in the outer asteroid belt. *Astron. J.*, **112**, 1278-1293.

Laskar, J. (1990). The chaotic motion of the Solar System. A numerical estimate of the size of the chaotic zones. *Icarus*, **88**, 266-291.

Laskar, J., C. Froeschlé and A. Celletti (1992). The measure of chaos by the numerical analysis of the fundamental frequencies. Applications to the standard mapping. *Physica D*, **56**, 253-269.

Lega, E. and C. Froeschlé (2001). On the relationship between fast Lyapunov indicator and periodic orbits for symplectic mappings. *Celest. Mech. Dynamical Astron.*, **81**, 129-147.

Lega, E., M. Guzzo and C. Froeschlé (2003). Detection of Arnold diffusion in Hamiltonian systems. *Physica D*, **182**, 179-187.

Lega, E., M. Guzzo and C. Froeschlé (2008). Diffusion in Hamiltonian qusi-integrable systems. *Lect. Notes Phys.,* **729**, 29-65.

Morbidelli, A. (2002). Modern Celestial Mechanics. Aspects of the Solar System Dynamics. Taylor and Francis, London.

Murray, C.D. and S.F. Dermott (1999). Solar System Dynamics. Cambridge University Press, UK.

Murray, N. and M. Holman (1997). Diffusive chaos in the outer asteroid belt. *Astron. J.*, **114**, 1246-1259.

Nesvorný, D. and S. Ferraz-Mello (1997). On the asteroidal population of the first-order Jovian resonances. *Icarus*, **130**, 247-258.

Nesvorný, D. and A. Morbidelli (1998). Three-body mean motion resonances and the chaotic structure of the asteroid belt. *Astron. J.*, **116**, 3029-3037.

Pilat-Lohinger, E. (2003). Eccentric orbits in double stars. Proceedings of the 3rd Austrian-Hungarian Workshop on Trojan and related Topics (Eds. F. Freistetter, R. Dvorak and B. Érdi), 35-45.

Quinlan, G.D. and S. Tremaine (1990). Symmetric multistep method for the numerical integration of planetary orbits. *Astron. J.*, **100**, 1694-1700.

Todorović, N., E. Lega and C. Froeschlé (2008). Local and global diffution in the Arnold web of a priori unstable systems. *Celest. Mech. Dynamical Astron.*, **102**, 13-27.

Tsiganis, K. (2008). Chaotic diffusion of asteroids. *Lect. Notes Phys.,* **729**, 111-150.

Villac, B.F. (2008). Using FLI maps for preliminary spacecraft trajectory design in multi-body environments. *Celest. Mech. Dynamical Astron.*, **102**, 29-48.

Wisdom, J. (1980). The resonance overlap criterion and the onset of stochastic behavior in the restricted three-body problem. *Astron. J.*, **85**, 1122-1133.